International Scientific Colloquium
Modelling for Electromagnetic Processing
Hannover, October 27-29, 2008

Control of free-surface instabilities during electromagnetic shaping of liquid metals

Ch. Karcher, V. Minchenya

Abstract

The present paper deals with the control and the damping of electromagnetically induced instabilities of free surfaces of liquid metals. Such instabilities occur under the effects of externally applied high-frequency magnetic fields. As a model configuration we consider a liquid metal drop subject to a high-frequency magnetic field. The control is managed by externally applying static magnetic fields that are known to damp fluid motion in electrically conducting liquids. Furthermore, we present a linear stability analysis that shows that the growth rates of surface instabilities are significantly reduced by the static magnetic field.

1. Introduction

The control of metal surfaces by electromagnetic forces is used in many metallurgical key technologies like levitation, cold crucible applications, and slit sealing [1], [2], [3]. In all these processes an applied high-frequency magnetic field is used to exert an electromagnetic pressure on the surface. This pressure shapes the surface. However, in application the stability of the free surface is a serious problem and surface control is crucial for success. Such electromagnetically induced instabilities were detected in a number of model experiments performed at TU Ilmenau [4]. For instance, it is observed that liquid metal drops start to oscillate whenever the high-frequency feeding current of the electromagnetic inductor exceeds a certain critical value [5]. The stability of a ring-type liquid metal surface is studied in [6]. Upon increasing the feeding current the initially flat surface undergoes a sequence of instabilities starting with the formation of small-amplitude capillary waves followed by large-amplitude static deformations. The wave number k of these deformations equals the reciprocal value of the skin depth δ, i.e. $k = 1/\delta$. Eventually the surface pinches. Finally, the stability of a disc-type surface is considered in [7]. It is observed that at a certain critical feeding current, a steady keyhole-type shape occurs. Upon a further increase, a transition to a cross-type shape takes place. At an even higher value, the disc is torn to pieces.

In addition, there are a number of analytical studies. In [8] and [9] it is demonstrated that an instability of a flat conducting free surface sets in when the applied alternating magnetic field exceeds a certain critical value. A linear stability analysis of a flat liquid metal surface between the thin gap of two parallel plates is performed in [10]. Based on both the Hele Shaw and the skin depth approximation the model predicts that a surface instability occurs when the destabilizing effect of the applied magnetic pressure exceeds the stabilizing effect of hydrodynamic pressure. However, it is incorrectly concluded that the most dangerous perturbations are characterized by a vanishing wave number. Another approach has been conducted in [11]. This analysis considers an infinitesimal thin electrically perfectly conducting liquid sheet that carries an electrical current directly along the edge. The result is a dispersion relation which is –except for a geometrical factor- identical to that in [10] when

the relation $k \propto 1/\delta$ is applied. However, by correcting [10], it is shown that the edge becomes unstable against perturbations of a certain range of wave numbers. Perturbations with smaller and larger wave numbers are stabilizes by gravity and surface tension.

In the present paper we investigate how such surface instabilities may be damped or even suppressed. As a first approach we extend the experimental investigations presented in [5] by superimposing a strong static magnetic. Moreover, we extend the stability analysis [10], [11] by taking into account the additional effect of a strong static magnetic field. It is well known that static magnetic fields generate Lorentz forces within a moving conducting liquid. These Lorentz forces exert a breaking effect on the fluid-flow, see [1], [2], [3]. The paper is organized as follows. In Sec. 2 we present results of model experiments. Sec. 3 shows the results of a linear stability analysis. Finally, we provide some main conclusions.

2. Model Experiments

2.1. Experimental Set-up

In the model experiments a drop of the low-melting liquid metal Galinstan is placed on a non-conducting water-cooled substrate. The high-frequency magnetic field is generated by a ring-type electromagnetic inductor consisting of 5 windings arranged in two layers. The inductor is fed by a high-frequency electrical current. The static magnetic field is generated either by a permanent magnet, see Fig. 1(a), or an electromagnet, see Fig. 1(b). Both arrangements allow to vary the field within the range $0 < B_{DC} < 100\text{mT}$. In case of the permanent magnet the field variation is established by changing the distance between magnet

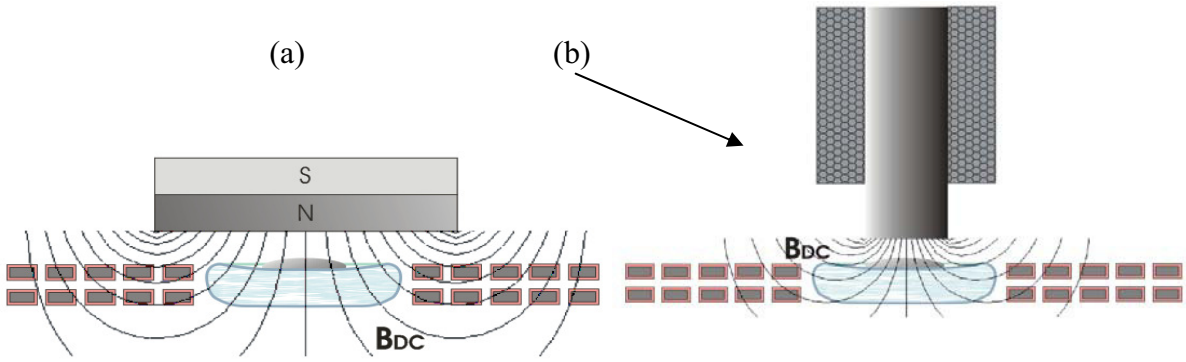

Fig. 1: Sketch of the experimental arrangement, (a) permanent magnet, (b) electromagnet.

and drop. On the contrary, the electromagnet is fixed in position and the field variation is established by changing the feeding DC current. However, both arrangements show some drawback. On the one hand, the positioning of permanent magnet distort the parameters of the LC-oscillator of AC generator leading to a change in both the applied AC current and AC frequency. On the other hand, the ferromagnetic material of the fixed electromagnet tend to amplify the AC magnetic field in the vicinity of the drop surface leading to higher values of the magnetic pressure. To evaluate these effects both methods to apply the static field were tested. During the experiments we fix the drop mass at $m = 10\text{g}$ and the applied AC inductor frequency at $f = 31\text{kHz}$ and gradually increase the AC current. The shape of the drop is recorded from below using a high-speed digital camera. Applying standard digital image processing to the recorded data we obtain the critical AC current I_C for the onset of drop oscillations. Moreover, we determine the mode numbers, the maximal amplitude A_{max}, and the growth rate λ of the oscillations. We repeat the experiment for various valued of B_{DC}.

2.2. Experimental Results

Fig. 2 shows for various mode numbers N the maximal amplitudes A_{max} of oscillations as a function of the applied AC current I for the case when the static magnetic field is absent, i.e. $B_{DC} = 0$. We observe that for all mode numbers A_{max} increases upon an increase of I. This is expected as the higher I the higher the magnetic pressure acting on the drop surface. Moreover, we observe that mode 2 shows the highest amplitudes. This mode corresponds to a cigar-type instability of the initially circular drop shape. The same behavior has already been detected in [5].

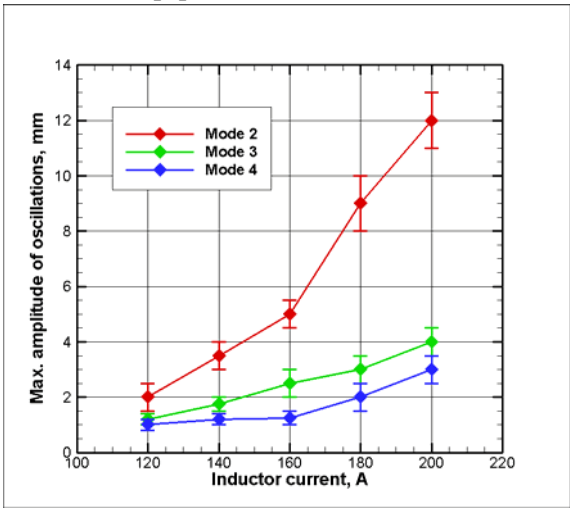

Fig. 2: A_{max} for various mode numbers as a function of the AC current for $B_{DC} = 0$.

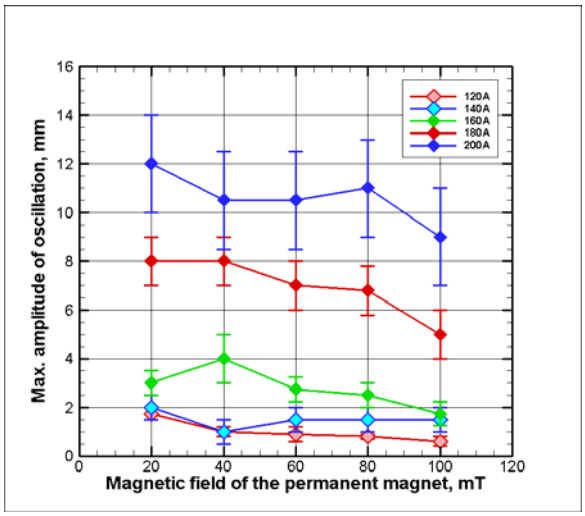

Fig. 3: A_{max} of mode 2 as a function of the DC field on permanent magnets.

Fig. 3 shows how the maximal amplitude of mode 2 depends on the DC field B_{DC} generated by the permanent magnet. We observe that for all applied AC currents the amplitudes slightly decrease upon increasing B_{DC}. We attribute this finding to the damping effect of a static magnetic field. However, our experiments show that even at a field strength of $B_{DC} = 100$mT the drop instability cannot be prevented. A similar behavior is found in the case when the static magnetic field is generated by an electromagnet. This is shown in Fig. 4. However, in this case, at fixed values of I and B_{DC}, the oscillation amplitudes are considerably higher than in the case when permanent magnets are applied. As mentioned above, this reflects the fact that the presence of the permanent magnet lead to a considerable distortion of the applied AC field and that the presence of the electromagnet intensifies the magnetic pressure acting on the drop surface.

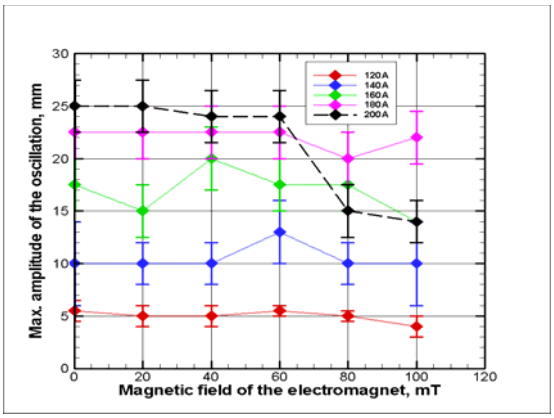

Fig. 4: A_{max} of mode 2 as a function of the DC field using electromagnet.

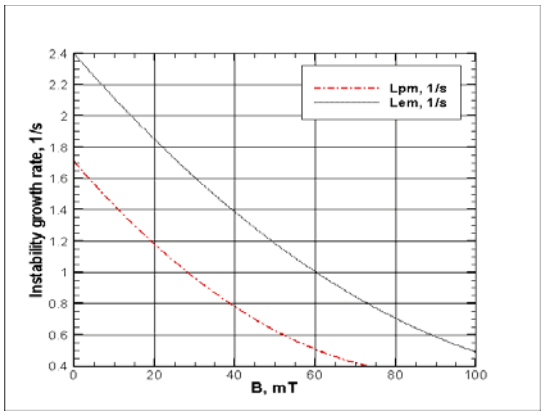

Fig. 5: Growth rate λ of mode 2 as a function of various DC fields.

Finally, Fig. 5 shows the exponential growth rates of mode 2. The graphs demonstrate that the growth rate can be considerably diminished when a strong static magnetic field is applied. For instance, for the case of a static field of $B_{DC} = 100$mT produced by an electromagnet, a reduction of 80% is observed, see black curve in Fig 5. Analysing the slope of this curve, we conclude that at even higher values of B_{DC}, the growth rate may relax to zero. We attribute this behavior to the damping effect of the static field. The corresponding growth rates for the case of the field produced by the permanent magnet are considerably smaller, see red curve in Fig. 5. Again, this behavior is explained by the distortion of the applied AC field by the permanent magnet and the intensifying effect of the electromagnet on the magnetic pressure acting on the drop surface.

3. Linear stability analysis

3.1. Analytical Model

We consider a similar arrangement as [7]. In this so-called Hele Shaw geometry the liquid metal is arranged in the gap of two parallel vertical plates of width 2d and of infinite height, see Fig. 6. The high-frequency magnetic field is generated by an inductor located at the distance z = L above the unperturbed interface. The inductor is fed by an alternating electrical

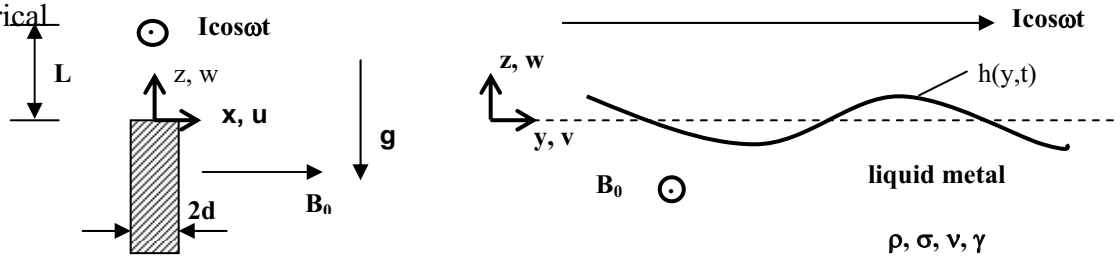

Fig. 6: Sketch of the geometric arrangement.

current Icosωt pointing in the y-direction. Hence, the induced magnetic vector potential is given by $\mathbf{A} = A(x,y,z;t)\,\mathbf{e}_y$. Moreover, the arrangement is submitted to homogeneous static magnetic field pointing in the x-direction, i.e. $\mathbf{B} = B\,\mathbf{e}_x$. The perturbed interface is described by the coordinate h(y,t). Liquid metal properties are density ρ, electrical conductivity σ, kinematic viscosity ν, and surface tension γ. The velocity field within the liquid metal is denoted by $\mathbf{u} = (u,v,w)$, where $u \equiv 0$. Gravity g is pointing in the negative z-direction.

3.2. Dispersion equation

In the following we focus the analysis to evaluate the effect of the applied static magnetic field. The Lorentz force density **f** that is generated within the liquid can be calculated using the equations

$$\mathbf{f} = \frac{1}{\rho}\left(\mathbf{j} \times \mathbf{B}\right),\ \mathbf{j} = \sigma\left[\mathbf{E} + \left(\mathbf{u} \times \mathbf{B}\right)\right] \qquad (2.1a,b)$$

Here, **j** denotes the induced eddy current density and **E** an applied electrical field. Assuming that the eddy currents flow in the y-z-plane only, we have $\mathbf{E} = 0$. Using $\mathbf{B} = B\mathbf{e}_x$ we obtain

$$\mathbf{f} = -\frac{\sigma}{\rho} B^2\left[v\,\mathbf{e}_y + w\,\mathbf{e}_z\right] \qquad (2.2)$$

As expected, the static magnetic field generates a breaking force within the moving liquid.

We now follow the analysis described in detail in [7]. The hydrodynamic problem is governed by the Hele Shaw equations including the electromagnetic force (2.2). The electrodynamic problem is governed by two Laplace equations for the y-component of the magnetic vector potential A. The equations are coupled via the Young Laplace equation that represents a pressure balance at the interface. This conditions writes as

$$z = h : p_M + p_a - p = \gamma \frac{\partial^2 h}{\partial y^2}\left(1 + (\partial h/\partial y)^2\right)^{-3/2},\ p_M = \frac{1}{2\mu_0}\left\langle\left(\nabla \times A\mathbf{e}_y\right)\right\rangle_{z=h}. \quad (2.3a,b)$$

Here, p_M, p_a, and p denote the magnetic pressure defined by equation (2.3b), the ambient pressure and the fluid pressure, respectively. We linearize the governing equations around the basic quiescent state characterized by an unperturbed interface and solve for the perturbed state characterized by an infinitesimally corrugated interface. Finally, introducing normal modes for the perturbed variables, by evaluating equations (2.3a,b) we eventually obtain the following dimensionless dispersion equation for interfacial disturbances.

$$\lambda^2 + 2\left(Ca + Ha^2\right)\lambda - k^2\left\{2Bo^2 - \left(k + 1/k\right)\right\} = 0. \quad (2.4)$$

Here, λ denotes the exponential complex growth rate and k represents the wave number. The parameters are the Bond number Bo, the Hartmann number Ha, and the capillary number Ca that measure the effects of the high-frequency magnetic field, the static magnetic, and friction relatively to the effect of surface tension. These parameters are defined by

$$Ca = \frac{\upsilon}{d^2}\left(\frac{\rho g^3}{\gamma}\right)^{-1/4},\ Ha^2 = \frac{\sigma}{2\rho}B^2\left(\frac{\rho g^3}{\gamma}\right)^{-1/4},\ Bo^2 = \frac{\mu_0 I^2}{2\pi^2 L^2}\frac{1}{(\rho g\gamma)^{1/2}}. \quad (2.5)$$

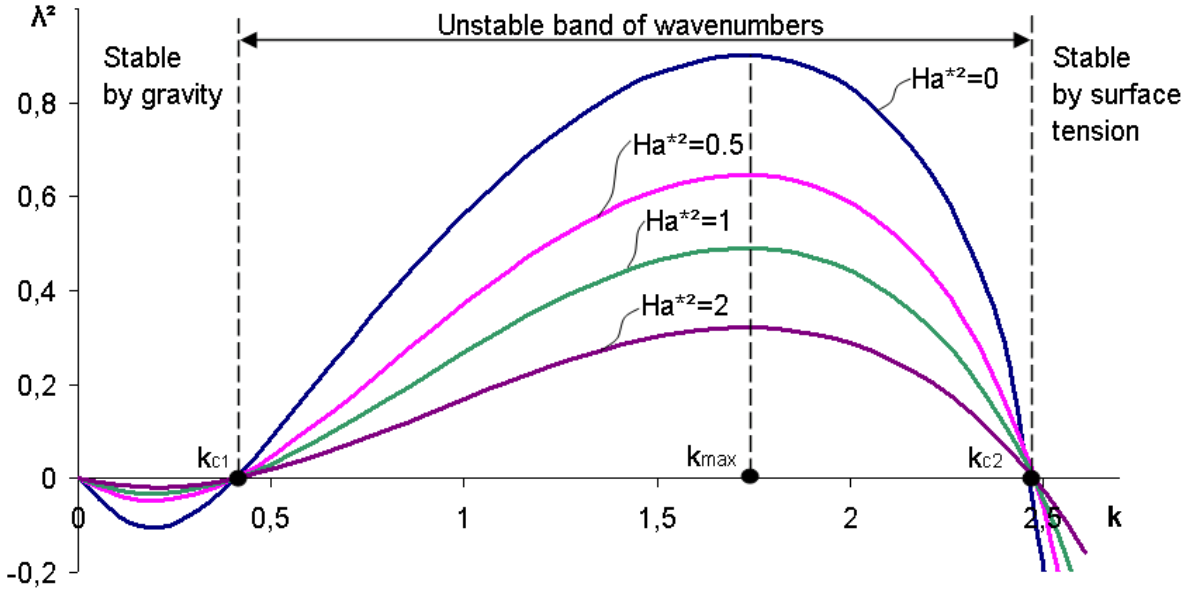

Fig. 7: Stability diagram

3.3. Stability diagram

Upon evaluating (2.4) we obtain that instability modes are characterized by a vanishing imaginary of the growth rate. The real part is given by

$$\lambda = -\left(\mathrm{Ca} + \mathrm{Ha}^2\right) + \sqrt{\left(\mathrm{Ca} + \mathrm{Ha}^2\right)^2 + \mathrm{k}^2\left\{2\mathrm{Bo}^2 - \left(\mathrm{k} + 1/\mathrm{k}\right)\right\}} \qquad (2.6)$$

From (2.6) we obtain a band of unstable wave numbers, the most critical wave number k_{max} that maximizes the growth rate, and the critical Bond number Bo_C. We find

$$\mathrm{Bo}^2 - \sqrt{\mathrm{Bo}^4 - 1} \le \mathrm{k} \le \mathrm{Bo}^2 + \sqrt{\mathrm{Bo}^4 - 1}\,,\ \mathrm{k}_{\max} = \tfrac{2}{3}\mathrm{Bo}^2 + \tfrac{2}{3}\sqrt{\mathrm{Bo}^4 - \tfrac{3}{4}}\,,\ \mathrm{Bo}_C = 1. \qquad (2.6a,b,c)$$

These values are independent of Ha. Thus the surface instability cannot be prevented by applying a static magnetic field. However, we find that the static magnetic field tends to decrease the growth rates. Fig. 7 shows the corresponding stability diagram. Here, the growth rate is plotted against the wave number for various values of the Hartmann number. Fig. 7 reflects again the earlier findings, namely that perturbations showing short and large wave numbers are stabilized by gravity and surface tension, respectively [11].

Conclusions and acknowledgements

We have investigated experimentally and analytical the effect of a strong static magnetic field on the instability of a liquid metal surface submitted to a high-frequency magnetic field. We find that the static field cannot prevent surface instabilities but can considerably damp their growth rates. This work is sponsored by the DFG under Research Grant KA-1660/3. We acknowledge support by Corus group. We thank J. Priede for helpful discussions.

References

[1] Y. Fautrelle: *Fluid flows induced by alternating magnetic fields*, in: Liquid metal magnetohydrodynamics, Eds: J. Lielpeteris and R. Moreau, Kluwer Academic Publishers, Dordrecht (1989).
[2] R. Moreau: *Magnetohydrodynamics*, Kluver, Dortrecht (1990).
[3] P. A. Davidson: *An introduction to magnetohydrodynamics,* Cambridge University Press (2002).
[4] Ch. Karcher, V. Kocourek: Free-surface instabilities during electromagnetic shaping of liquid metals, PAMM, 2008 (in press).
[5] V. Kocourek, Ch. Karcher, M. Conrath, D. Schulze, Stability of liquid metal drops affected by a high-frequency magnetic field, Phys. Rev. E Vol. 74, 026303 (2006).
[6] J.U. Mohring, Ch. Karcher, D. Schulze: Stability of a liquid metal interface affected by a high-frequency magnetic field, Phys. Rev. E. 71, 301-306, 2005.
[7] M. Conrath, Ch. Karcher: Behavior of a liquid metal disc in a magnetic field of a circular current loop; paper for 5th International Symposium EPM2006, Sendai, Japan, 210-213, 2006.
[8] Y. Fautrelle, A. Sneyd: *Instability of a plane conducting free surface submitted to an alternating magnetic field*, J. Fluid Mech. (1998), **375**, pp. 65-83.
[9] Y. Fautrelle, J. Etay, S. Daugan: *Free surface horizontal waves generated by low frequency alternating magnetic fields,* J. Fluid Mech. **527**, 285-301, (2005).
[10] Ch. Karcher, J.-U. Mohring: Stability of a liquid metal interface affected by a high-frequency magnetic field, Magnetohydrodynamics 29, 267-276, (2003).
[11] J. Priede, J. Priede, J. Etay, Y. Fautrelle: Edge pinch instability of liquid metal sheet in a transverse high-frequency ac magnetic field. Physical Review E, Vol. 73, 066303 (2006).

Authors

Priv.-Doz. Dr.-Ing. habil. Christian Karcher
Fachgebiet Thermo- und Magnetofluiddynamik
Technische Universität Ilmenau
P.O. Box 10 05 65
D-98684 Ilmenau, Germany
E-mail: christian.karcher@tu-ilmenau.de

Dr-Ing. Vitaly Minchenya
Fachgebiet Thermo- und Magnetofluiddynamik
Technische Universität Ilmenau
P.O. Box 10 05 65
D-98684 Ilmenau, Germany
E-mail: vitaly.minchenya@tu-ilmenau.de